Hrvatski meteorološki časopis, 37, 63-78, 2002.

UDK: 551.515
Stručni rad

A MODELLING STUDY OF THE UNIVERSAL STABILITY FUNCTIONS IN SIMPLE NUMERICAL MODEL SIMULATIONS OVER IDEALIZED URBAN SURFACE

Ispitivanje univerzalnih funkcija sličnosti jednostavnim numeričkim modelima nad idealiziranom urbanom površinom

MAJA TELIŠMAN PRTENJAK[1], MERIEM ZITOUNI[2] and LIDIJA SRNEC[2]

[1] Andrija Mohorovičić Geophysical Institute, Faculty of Science, University of Zagreb
Horvatovac bb, 10000 Zagreb, Croatia

[2] Meteorological and Hydrological Service, Grič 3, Zagreb, Croatia

telisman@rudjer.irb.hr

Primljeno 19. veljače 2001, u konačnom obliku 23. siječnja 2003.

ABSTRACT: The aim of this numerical study is to evaluate several formulations of universal stability functions, which characterise turbulent exchange processes in the surface layer in the simple one-dimensional and two-dimensional numerical models. In the first part of the paper, the one-dimensional prognostic model illustrates the basic behaviour of the stability functions and in the second part, the ability of the mentioned functions to provide a physical and numerical successful two-dimensional integration of the urban heat island circulation is examined. The results show that the examined formulations did not succeed in describing the development of the urban heat island circulation.

Key words: Monin-Obukhov similarity theory, turbulent eddy coefficients for momentum and heat, urban heat island circulation

SAŽETAK: U ovoj numeričkoj studiji pokušalo se procijeniti nekoliko oblika univerzalnih funkcija sličnosti, koji opisuju turbulentne procese miješanja u površinskom sloju, jednostavnim jednodimenzionalnim i dvodimenzionalnim numeričkim modelom. U prvom dijelu ove studije, jednodimenzionalni prognostički model pokazuje osnovne karakteristike univerzalnih funkcija stabilnosti, a u drugom dijelu se ispituje njihova fizikalna i numerička sposobnost u dvodimenzionalnim simulacijama da reproduciraju cirkulaciju urbanog toplinskog otoka. Rezultati su pokazali da spomenute funkcije nisu uspjele opisati razvoj cirkulacije urbanog toplinskog otoka na zadovoljavajući način.

Ključne riječi: Monin-Obukhovljeva teorija sličnosti, koeficijenti turbulentne izmjene količine gibanja i topline, cirkulacija urbanog toplinskog otoka

1. INTRODUCTION

Although the Monin-Obukhov similarity theory (MOST) and *K*-theory have a number of difficulties and limitations, they have been widely exploited for the parameterisation of surface layer fluxes for the numerical modelling purpose. It is well known that MOST works only when the winds are not calm, in another words, when friction velocity is not zero. Also, MOST is a semiempirical theory and universal functions are obtained by a unique set of measurements over homogeneous surfaces and statistical estimates and they are appropriate to a given

place. These are some of the reasons for a number of proposed universal stability functions derived by many authors (e.g. Businger *et al.*, 1971; Louis, 1979; Högström, 1988; Cvitan, 1991; Delage and Girard, 1992; Delage, 1997; Weidinger *et al.*, 2000).

For the statically unstable boundary layer two types of stability functions are most frequently used: the (-1/2) power-low profile approximation (which leads to a non-physical increase in sensible heat flux as friction velocity (u_*) $\longrightarrow 0$ and does not satisfy MOST completely) and the (-1/3) power-low profile approximation that describes the free convection case and exhibits a well behaved flux dependence upon u_*. Recently, the latter shape of the stability functions for the free convection case, proposed by Delage and Girard (1992), has been successfully implemented in the global atmospheric circulation model (ACM) run at the Canadian Meteorological Centre in combination with the formulation of Delage (1997) for the stable case. For the unstable case the proposals are:

$$\varphi_H(z/L) = \left(1 - c\frac{z}{L}\right)^{-1/3} \quad (1)$$

$$\varphi_M(z/L) = \left(1 - c\frac{z}{L}\right)^{-1/6} \quad (2)$$

and for stable case (based on the formulation developed by Louis, 1979):

$$\varphi_H(z/L) = \varphi_M(z/L) = 1 + 12\frac{z}{L} \quad (3)$$

where φ_H and φ_M are the stability functions for heat and momentum, c is an empirical constant and L is Monin-Obukhov length. Their suggestions for both the unstable and stable cases demonstrated a consistency with both the free convection and surface layer definition. They can be also applied to the whole boundary layer. Their simplicity also makes them rather attractive.

Delage and Taylor (1970) tried to simulate a mesoscale phenomenon – an idealised nighttime urban heat island circulation. Although they used K-coefficients as a function of height, their model had difficulties in the simulation of urban circulation. The question that appears is how the above-mentioned physically correct proposals can improve the simulation of a turbulent exchange process in a simple two-dimensional numerical model. For this purpose, a mesoscale model, which can be regarded as derived from the Delage and Taylor (1970), has been used. Therefore, the objective of the present paper is to evaluate equations 1–3, which characterise turbulent exchange processes, in the simple one-dimensional (1-D) and two-dimensional (2-D) prognostic numerical models. In the first part of the paper, the 1-D model is designed to increase understanding of the behaviour of the stability functions represented by equations 1–3. In the second part, the ability of the mentioned functions to provide a successful physical and numerical integration of the urban heat island circulation is examined.

2. THE BASIC MODELS' EQUATIONS

The models involve three prognostic equations governing the evaluation of the horizontal wind components u and v in the x and y directions, and of the potential temperature, Θ

$$\frac{\partial u}{\partial t} = -u\frac{\partial u}{\partial x} - w\frac{\partial u}{\partial z} - \frac{R\Theta}{p}\left(\frac{p}{p_0}\right)^{(R/Cp)}\frac{\partial p}{\partial x} + fv + \frac{\partial}{\partial z}\left(K_{ZM}\frac{\partial u}{\partial z}\right) + K_{XM}\frac{\partial^2 u}{\partial x^2} \quad (4)$$

$$\frac{\partial v}{\partial t} = -u\frac{\partial v}{\partial x} - w\frac{\partial v}{\partial z} - fu + \frac{\partial}{\partial z}\left(K_{ZM}\frac{\partial v}{\partial z}\right) + K_{XM}\frac{\partial^2 v}{\partial x^2} \quad (5)$$

$$\frac{\partial \Theta}{\partial t} = -u\frac{\partial \Theta}{\partial x} - w\frac{\partial \Theta}{\partial z} + \frac{\partial}{\partial z}\left(K_{ZH}\frac{\partial \Theta}{\partial z}\right) + K_{XH}\frac{\partial^2 \Theta}{\partial x^2} \quad (6)$$

The symbols used are the conventional ones used in meteorology. Density in Equation 4 is described by pressure and potential temperature. In order to devise physically realistic numerical models of turbulent transfer processes, which are the dominant factors in the formation of the heat island circulation, the vertical eddy diffusivity for momentum and heat is used

according to the K-theory. The details of the K_{ZM} and K_{ZH} physical parameterisation will be discussed later. The computational diffusion coefficients for momentum (K_{XM}) and heat (K_{XH}) are equal, and are used in the 2-D model. Humidity is omitted in the models.

The continuity equation is in an incompressible form and the vertical velocity (w) is calculated from:

$$\frac{\partial u}{\partial x}+\frac{\partial w}{\partial z}=0 \tag{7}$$

In the models, the hydrostatic assumption is used which yields the equation for pressure:

$$\frac{\partial p}{\partial z}=-\frac{pg}{R\Theta}\left(\frac{p_0}{p}\right)^{(R/Cp)} \tag{8}$$

According to previous studies about urban heat island circulation, due to relatively small vertical accelerations in the urban area this assumption is reasonable (e.g. Vukovich *et al.*, 1976).

Equations 4–8 are the basic equations governing the dynamics and thermodynamics in both the 1-D and 2-D models.

3. RESULTS OF NUMERICAL SIMULATIONS WITH THE ONE-DIMENSIONAL MODEL

3. 1. One-dimensional (1-D) model

The 1-D model has a staggered grid because staggering increases the effective resolution, according to Pielke (1984) among others. The model has only the vertical coordinate with a constant vertical grid interval (Δz = 20 m), where the origin of the grid system is situated at the ground and the top of the model domain at $z(N) = H$. The co-ordinates of the vertical grid points for u, v, and Θ are denoted by z (i) and for K_{ZM} and K_{ZH} by zm (i). These two grid discretizations are connected in such a way that zm (i) is equal to z (i-$1/2$) and zm (i+1) to z (i+$1/2$) (see Fig. 1).

To design the 1-D prognostic model, several approximations have been used:

a) only temporal and vertical changes are retained in the model,
b) subsidence is neglected,
c) gradient pressure force is omitted.

Finally, the model's Equations 4–7 are:

$$\frac{\partial u}{\partial t}=fv+\frac{\partial}{\partial z}\left(K_{ZM}\frac{\partial u}{\partial z}\right) \tag{9}$$

$$\frac{\partial v}{\partial t}=-fu+\frac{\partial}{\partial z}\left(K_{ZM}\frac{\partial v}{\partial z}\right) \tag{10}$$

$$\frac{\partial \Theta}{\partial t}=\frac{\partial}{\partial z}\left(K_{ZH}\frac{\partial \Theta}{\partial z}\right) \tag{11}$$

where $f = 10^{-4}$ s^{-1}, and their finite difference analogs are given in Appendix A.

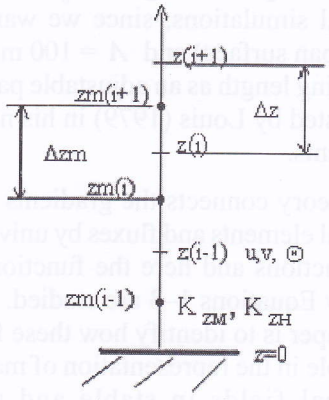

Figure 1. A schematic staggered grid for computation of u, v, Θ, K_{ZM}, K_{ZH}. Values of u, v and Θ are defined at z (i) points, whereas values of K_{ZM}, K_{ZH} are defined at zm (i) (i.e. z (i-1/2)) grid points. The vertical grid interval Δz is equal to Δzm.

Slika 1. Shematski prikaz razmaknute mreže za proračun u, v, Θ, K_{ZM}, K_{ZH}. Vrijednosti u, v i Θ definirane su u z (i) točkama, a vrijednosti K_{ZM}, K_{ZH} su definirane u zm (i) (što odgovara točkama mreže z (i-1/2)). Vertikalni korak mreže Δz jednak je Δzm.

One of the main difficulties in modelling turbulent processes in a planetary boundary layer is specifying the expression for K_{ZM} and K_{ZH}. The vertical fluxes are evaluated using the K-theory and theirs expressions are as follows:

$$K_{ZM}=\left(\frac{l}{\varphi_M}\right)^2\left|\frac{\partial V}{\partial z}\right| \tag{12}$$

and $$K_{ZH} = \frac{l^2}{\varphi_M \varphi_H} \left| \frac{\partial V}{\partial z} \right| \quad (13)$$

where $k = 0.4$ and $|V|^2 = u^2 + v^2$ (Delage, 1997). The mixing length (l) is based on two empirical considerations. Inside the surface layer (h), l is linear with height and above it l approaches Λ. Among several expressions for l that have been suggested we use those introduced by Blackadar (1962). They are given by:

$$l = \begin{cases} kz & z < h \\ \dfrac{k(z+z_0)}{1 + \dfrac{k(z+z_0)}{\Lambda}} & z \geq h \end{cases} \quad (14)$$

and with a roughness length of z_0=1 m (in these numerical simulations, since we want to describe urban surface) and Λ = 100 m (asymptotic mixing length as an adjustable parameter) as suggested by Louis (1979) in his numerical experiments.

The K-theory connects the gradients of meteorological elements and fluxes by universal stability functions and here the functions represented by Equations 1–3 are studied. The goal of this paper is to identify how these functions are reliable in the representation of main meteorological fields in stable and unstable conditions, in the simple 1-D model compared against other K-profile formulations.

We have used the relationship valid in the surface layer according to Delage and Girard (1992) and Delage (D97 hereafter)

$$\frac{z}{L} = \frac{\varphi_M^2}{\varphi_H} Ri$$

Since $z/L \sim Ri$ (Richardson number), the functions are transformed from $\varphi(z/L)$ into $\varphi(Ri)$ because Delage and Girard (1992) pointed out the appropriateness of using functions of Ri. This allows a matching between the surface and Ekman layer, and they can be easily applied to the whole boundary layer. Therefore, our functions (Eqs. 1–3) become, for stable conditions:

$$\varphi_M = \varphi_H = 1 + 12Ri \quad (15)$$

and the K-profiles are:

$$K_{ZM} = K_{ZH} = l^2 \frac{\left| \frac{\partial V}{\partial z} \right|^5}{\left[\left| \frac{\partial V}{\partial z} \right|^2 + 12 \frac{g}{\Theta} \frac{\partial \Theta}{\partial z} \right]^2} \quad (16)$$

for non-critical Ri or R_f. Delage (1997) tried to derive a formulation for K_z as simple as possible for global ACM, but keeping an acceptable level of complexity. He mentioned that, because of the variability within the grid box, there are regions with intermittent or patchy turbulence even if Ri is super-critical. Thus, Equation 16 is designed to maintain some (residual) transfer at values of Ri around 1.0.

In the unstable case, where c = 40, it is valid:

$$\varphi_M = (1 - 40Ri)^{-1/6}$$
$$\varphi_H = (1 - 40Ri)^{-1/3} \quad (17)$$

$$K_{ZM} = l^2 \left(\left| \frac{\partial V}{\partial z} \right|^3 - \frac{40g}{\Theta} \frac{\partial \Theta}{\partial z} \left| \frac{\partial V}{\partial z} \right| \right)^{1/3} \quad (18)$$

$$K_{ZH} = l^2 \left(\left| \frac{\partial V}{\partial z} \right|^2 - \frac{40g}{\Theta} \frac{\partial \Theta}{\partial z} \right)^{1/2} \quad (19)$$

In their numerical study of heat island circulation, Delage and Taylor (1970) used K-formulations based on the 'mixing-length formulation' and they did not succeed in simulating the urban circulation in a completely realistic way. Since a new formula will be applied for the same problem, the formulations from Delage and Taylor (1970) (D70 hereafter) are:

$$K_{ZM} = K_{ZH} = \begin{cases} l^2 \left(\left| \frac{\partial V}{\partial z} \right| - \frac{18 \cdot (gl)^{1/2}}{\Theta} \frac{\partial \Theta}{\partial z} \right) & \frac{\partial \Theta}{\partial z} \leq 0 \\ l^2 \dfrac{\left| \frac{\partial V}{\partial z} \right|^2}{\left| \frac{\partial V}{\partial z} \right| + \frac{18 \cdot (gl)^{1/2}}{\Theta} \frac{\partial \Theta}{\partial z}} & \frac{\partial \Theta}{\partial z} > 0 \end{cases} \quad (20)$$

where Equation 14 has been compared with Equations 16, 18 and 19 in the 1-D model. For a further comparison constant K-profiles ($K_{ZH} = 1.35 K_{ZM}$) have been added and O'Brien's $K(z)$-profile which is a cubic polynomial (O'Brien, 1970):

$$K_{ZM} = K_{ZM}(z_i) + \left[\frac{(z_i - z)}{(z_i - h)}\right]\left\{K_{ZM}(h) - K_{ZM}(z_i) + (z-h)\left[\left(\frac{\partial K_{ZM}}{\partial z}\right)_h + \frac{2(K_{ZM}(h) - K_{ZM}(z_i))}{(z_i - h)}\right]\right\} \quad (21)$$

where $K_{ZM}(z_i)$ and $K_{ZM}(h)$ are eddy coefficients at the planetary boundary layer height (z_i) and the surface layer height. The advantage thereof is a quite physical realistic profile with a maximum about (1/3) of the height of the boundary layer. The deficiency of this profile is in the *a priori* knowledge of h, z_i, $K_{ZM}(z_i)$ and $K_{ZM}(h)$.

Near the top of the entrainment layer, turbulence is very small and $K_{ZM}(z_i)$ is assumed arbitrary as 0.05 m^2s^{-1}, while $K_{ZM}(h)$ is computed from the expression:

$$K_{ZM}(h) = l^2\left|\frac{\partial V}{\partial z}\right|$$

Using Equation 21, K_{ZH} is obtained by multiplying K_{ZM} with 1.35. According to Stull (1988), there is some experimental evidence to suggest that for statically neutral conditions (K_{ZH}=1.35K_{ZM}) is valid. We believe that for these numerical simulations, this approximation is reasonable, when it is not possible to calculate K_{ZH} directly.

Boundary conditions are:
At $z = 0$; $u = 0$, $v = 0$, friction velocity (u_*) = 0.3 ms^{-1}, z_0 = 1m, $K_{ZM} = 0.4\, u_* z_0 = 0.12$ m^2s^{-1}, K_{ZH} = $1.35 \cdot 0.4\, u_* z_0 = 0.16$ m^2s^{-1} (except for the K-constant case); Θ_0 = 285.65 K, h = 100 m, z_i =1000 m.

At $z = H$ = 2400 m, Θ_H = 287.95 K,

$$\frac{\partial u}{\partial z} = \frac{\partial v}{\partial z} = \frac{\partial \Theta}{\partial z} = \text{constant.}$$

Initial conditions are:

At $t = 0$, $v = 0$, $\quad \frac{\partial \Theta}{\partial z} = \left(\frac{\partial \Theta}{\partial z}\right)_o = (2^0/1000\text{m})_0$

from the top toward the bottom of the model domain.

z_i and h are defined *a priori* and they divide the model domain in three parts. In the surface layer, the initial wind profile is log-linear for a u-component while in the upper part u = constant. Time integration lasts 28 hours with a time step Δt = 1 s. At the initial time, the potential temperature gradient describes a stable atmosphere. Between the ground and the first model levels, unstable conditions are set because they are chosen to simulate a warm urban area at night.

In these numerical simulations four different parameterisations for K-profiles are used inside the planetary boundary layer. Firstly, the K-constant case is integrated with K_{ZM} = 50 m^2s^{-1}. Secondly, the numerical simulations imply Equations 14, 16, 18 and 19 for the D97 case, thirdly, Equations 14 and 20 are used (D70 case), and, finally, O'Brien's K (z)-profile is integrated (Eq. 21). In the free atmosphere, turbulence is neglected, and this is valid for all numerical simulations. The profiles of potential temperature and wind components are analysed together with K_{ZM}, K_{ZH} and they are shown for 40 minutes, 3 and 12 hours.

3. 2. 1-D model results

Figure 2a displays four different K-cases after three hours of time integration tested on the same initial case. In this figure, only the first 1400 m height is included although the complete grid network actually extends to 2400 m height. At first glance, O'Brien's and D70 profiles give similar results while D97 formulations give values that approach constant K-profiles. Higher K-values in D97 and the constant K-cases represent more pronounced turbulent processes and enhanced surface fluxes. In the former case, K_{ZH} values are almost doubled compared to the K_{ZM} case. Therefore, u, v and Θ -profiles are more mixed inside the boundary layer (Figs. 2b, 2c). In the K-constant case there is no interaction between the K-coefficient and both wind and potential temperature fields. In this case, the strongest convergence of u and v-field values toward 0 ms^{-1} and the potential temperature profile toward adiabatic can be observed (not shown). It is important to stress that the D97 case gives much higher K_z values compared to the D70 case, especially in the K_{ZH}.

In these numerical simulations we do not compare the profiles of wind and potential temperature with the observed ones. Direct comparison between 1-D model results and observations is always difficult due to factors such as advection, varying synoptic wind and gravity waves. In these idealised numerical simulations, the aim is to present the characteristics and dif-

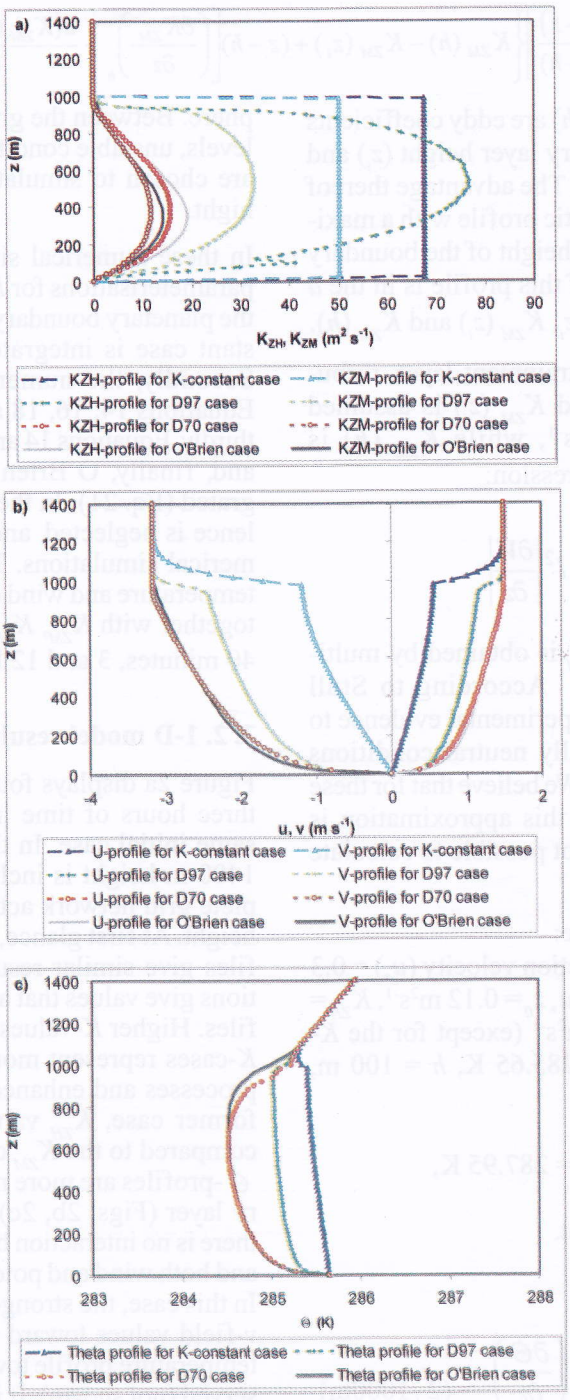

Figure 2. Results by one-dimensional model after 3 hours of time integration for constant *K*-profile (long-dashed line with triangles); *K*-profiles represented by Equations 16, 18 and 19 (short-dashed line with crosses); *K*-profiles represented by Equation 20 (short-dashed line with circles) and O'Brien *K*-profiles (Eq. 21) (solid line). a) K_{ZM} ($m^2 s^{-1}$) and K_{ZH} ($m^2 s^{-1}$); b) *u* and *v* wind components (ms^{-1}); c) potential temperature Θ (K).

Slika 2. Rezultati jednodimenzionalnog modela nakon 3 sata vremenske integracije za konstantni *K*-profil (dugocrtkana linija s trokutićima); *K*-profil predstavljen jednadžbama 16, 18 i 19 (kratkocrtkana linija s križićima); *K*-profil predstavljen jednadžbom 20 (kratkocrtkana linija s kružićima) i O'Brienov *K*-profil (jednadžba 21 (puna linija). a) K_{ZM} ($m^2 s^{-1}$) i K_{ZH} ($m^2 s^{-1}$); b) *u*- i *v*-komponente vjetra (ms^{-1}); c) potencijalnu temperaturu (K).

ferences of the u, v, Θ and K_Z profiles for the same initial conditions above an urban area.

Figure 3 depicts the vertical distribution of the change in eddy coefficients, wind field and potential temperature for the D97 case after 40 minutes, 3 and 12 hours of time integration. In Figure 3a, K-coefficients show the evolution of the turbulent exchange processes from the surface. As it was already mentioned, the K_{ZH} values are almost always twice as high as K_{ZM} values. The characteristics of the wind are more complex because of the Coriolis force; in the free atmosphere the u-component, for example, decreases in time with a simultaneous increase of the v-component (Fig. 3b). An inertial oscillation develops in the u and v-field and the amplitude of the disturbance is 3.5 ms^{-1}. This behaviour is somewhat different in the boundary layer where intensive turbulent processes are included.

When included in the equations, turbulence evidently limits the magnitude of the u and v wind components. Only at large z values, where turbulent effects are reduced, the Coriolis effect has an apparent maximum. A time-dependent decrease in the wind field follows a decrease in the K-coefficients. An initial potential temperature profile changes considerably in time, converging toward a very well mixed profile (Fig. 3c).

A smaller vertical resolution showed very similar results.

4. RESULTS OF NUMERICAL SIMULATIONS WITH THE TWO-DIMENSIONAL MODEL

4. 1. Two-dimensional (2-D) model

The 2-D prognostic model derived here can be regarded as derived from the Delage and Taylor (1970) model, although there are differences not only in the equations (here, the Coriolis effect is included) but also in the finite difference schemes. The model domain is in an x-z plane and full Equations 4–8 are used. According to Delage and Taylor (1970), when there is no synoptic wind in the system, it is sufficient to study one half of the urban heat island circulation due to the symmetry between two cells above the city. Therefore, the same model domain and boundary condition were used as in the Delage and Taylor (1970) model in order to make the comparison of model results easier. Without gradient wind in the model, above the urban centre ($x = 0$), only convection is important. The horizontal advection effects, which can be neglected, are described through the boundary conditions.

The boundary conditions are as follows:
At $x = 0$, $u = v = 0$;

At $x = L$, $\frac{\partial \Theta}{\partial x} = \frac{\partial u}{\partial x} = \frac{\partial v}{\partial x} = 0$;

At $z = z_0$, $u = v = w = 0$ and $\Theta = \Theta_s$ (x,t). To describe the urban area, z_{0u} is set to 1.0 m, while for a rural area $z_{0r} = 0.1$ m (Stull, 1988).

At $z = H$, $\frac{\partial u}{\partial z} = 0$, $\frac{\partial v}{\partial z} = 0$, p_H = constant and Θ_H = constant.

The initial conditions are as follows:

At $t = 0$, $u = 0$, $v = 0$, $\frac{\partial \Theta}{\partial z} = \left(\frac{\partial \Theta}{\partial z}\right)_o$ and the urban heat island grid points have the initial potential temperature (Θ_u) $\Theta_u = \Theta_r + \Delta\Theta_s$; that is composed by the initial rural potential temperature (Θ_r) and the heat island intensity ($\Delta\Theta_s$).

The solution is obtained by discretizing Equations 4–8 using finite differences. A constant horizontal grid (Δx) has a value of 1000 m and a constant Δz is 100 m, although some numerical experiments with variable vertical grid interval were performed. Advection terms in the 2-D model are approximated by the upstream difference scheme and diffusion terms by the second-order central differences with a 75% implicit scheme. The Coriolis terms are calculated by an implicit scheme; the updated value for u from Equation 4 is used in Equation 5 for the v-component (see Pielke, 1984). The quantity w is determined from Equation 7. Equations 4–8 in finite-difference form with a variable vertical grid interval are derived in Appendix B. The forward explicit two-time level scheme which is used in the model, is the simplest time-scheme but with a small range of stability (Kalnay and Kanamitsu, 1988). Therefore, we use horizontal diffusion, although the used advection scheme is a damping one.

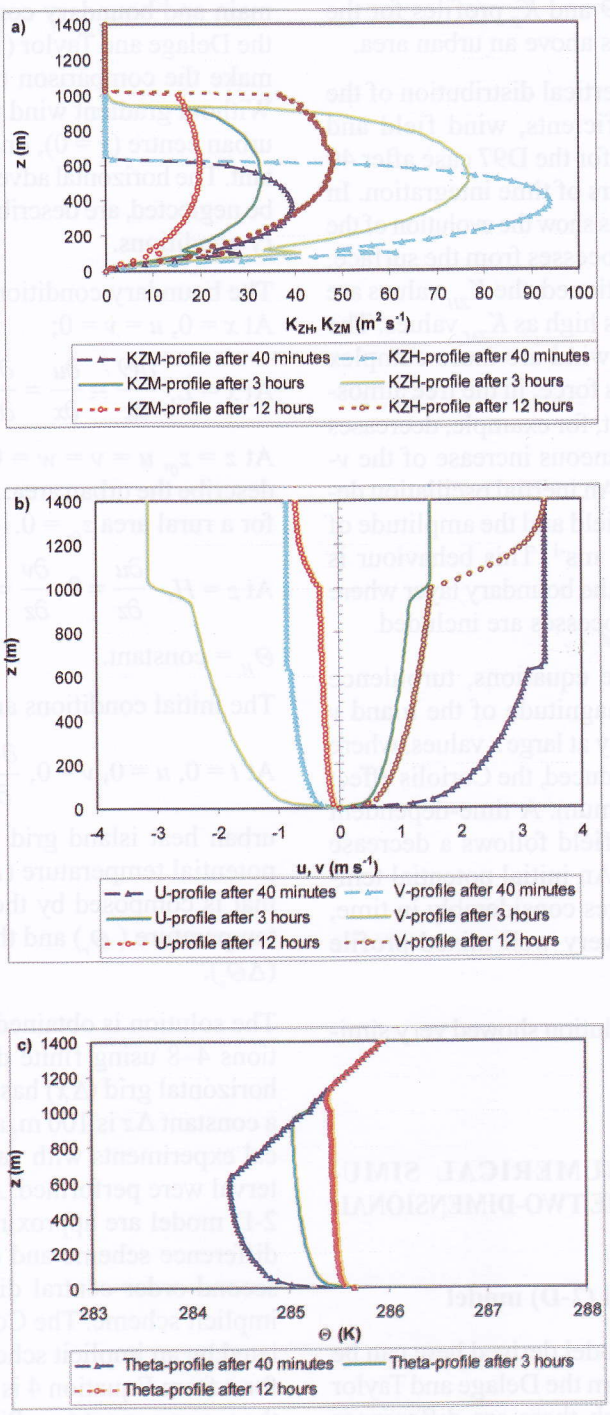

Figure 3. Results by 1-D model for stability functions and *K*-profiles represented by Equations 16, 18 and 19 for 40 minutes (long-dashed line with triangles); 3 hours (bold solid line) and 12 hours (short-dashed line with circles) for a) K_{ZM} ($m^2 s^{-1}$) and K_{ZH} ($m^2 s^{-1}$); b) *u* and *v* wind components (ms^{-1}); c) potential temperature Θ (K).

Slika 3. Rezultati jednodimenzionalnog modela za funkcije stabilnosti i *K*-profil predstavljen jednadžbama 16, 18 i 19 za 40 minuta (dugocrtkana linija s trokutićima); 3 sata (puna linija) i 12 sati (kratkocrtkana linija s kružićima) za a) K_{ZM} ($m^2 s^{-1}$) i K_{ZH} ($m^2 s^{-1}$); b) *u*- i *v*-komponente vjetra (ms^{-1}); c) potencijalnu temperaturu (K).

In the first part of the next paragraph, the *K*-constant case will be performed while in the second part, for the vertical *K*-coefficients, the formulas 16, 18 and 19 with Equation 14 for the mixing length definition will be used.

4. 2. 2-D model results with K- constant

Additional details of the model configuration in the case of the constant $K_{ZM} = K_{ZH} = 50$ m^{2}s^{-1} are given in the Table 1. In the model, synoptic winds are absent and an idealised heat island circulation at night with anticyclonic conditions is studied.

Since in the model the urban heat island intensity is only a mechanism responsible for the circulation above the urban and rural areas, after approximately 3 hours of numerical integration a steady state is attained. Figures 4 and 5 show the main characteristics of the wind velocity and potential temperature fields, respectively. For clarity of presentation, a fraction of the computational domain is omitted. The model domain in the figures is reduced to $0 \text{ m} \le x \le 11000$ km and $0 \text{ m} \le z \le 2100$ m.

Table 1.: Specifications for the two-dimensional numerical simulations.

Tablica 1.: Konstante i ulazni parametri korišteni u dvodimenzionalnim numeričkim simulacijama.

Constants:	
Horizontal eddy transfer coefficient for momentum and heat ($K_{XM} = K_{XH}$)	50 m^{2}s^{-1} (or 100 m^{2}s^{-1})
Reference surface pressure (p_o)	1000 hPa
Coriolis parameter (f)	10^{-4}s^{-1}
Specific gas constant for dry air (R)	287 J kg^{-1}K^{-1}
Specific heat at constant pressure (Cp)	1004.6 J kg^{-1}
Acceleration due to gravity (g)	9.81 ms^{-2}
Input parameters:	
Width of the model domain (L)	20 000 m
Top of the model domain (H)	2 400 m
Heat island boundary (x_a)	5 000 m
Initial temperature gradient $(\partial\Theta/\partial z)_o$	0.002 Km^{-1}
Rural surface potential temperature (Θ_r)	10°C
Urban surface potential temperature (Θ_u)	12.5°C
Constant upper boundary pressure (p_H)	755 hPa
Rural roughness lenght (z_{or})	1.0 m
Urban roughness lenght (z_{ou})	0.1 m
Weight parameter for current contribution (β_1)	0.25
Weight parameter for future contribution (β_2)	0.75

After 40 minutes of time integration, the main characteristics of wind velocity components are depicted in Figures 4a–4c. Above the heat island boundary ($x = x_a$), the urban circulation, which is of a relatively small horizontal and vertical extent at the beginning of the integration, is growing. In Figure 4a, in the *u*-component, a zone of convergence is established above the urban part. The strongest winds of ~ 1.5 ms^{-1} are at a height of approximately 100 m. Above 600 m there is a well-defined return flow toward the rural area. Its maximum value is ~0.5 ms^{-1} at 1000 m height. In Figure 4b, the mentioned low-level convergence influences upward motions (~ 0.2 ms^{-1}). These upward motions near the urban centre are accompanied by a subsidence (-0.1 ms^{-1}) over larger rural areas that close a circulation cell. The dependence of the Coriolis force on the circulation is visible in Figure 4c. The winds rotate in the expected clockwise sense at all heights under the influence of the Coriolis deflection. At the same time, a strong horizontal temperature gradient occurs at $x = x_a$ (Fig. 4d). As the urban circulation develops, advection of the colder rural air toward the urban part changes the Θ-field. Low-level winds affect the position of the initial horizontal temperature gradient, moving it toward the urban centre. The effect of the vertical velocities is also visible in Figure 4d, carrying the warmer urban air at higher altitudes.

After ~3 hours of time integration, the main characteristics of the wind velocity components for the steady state circulation are depicted in Figures 5a–5c. In Figure 5a, the heat island circulation is very well developed with the strongest winds of ~1.5 ms^{-1} (at 200 m height) and with a two-times weaker return flow of ~0.8 ms^{-1} (at 1000 m height). The largest vertical velocities (0.25 ms^{-1}) can be found above the centre of the urban area at $z = 700$ m (Fig. 5b). The effect of the Coriolis deflection is now more pronounced, since circulation has been developing for some time. Isolines of the Θ-field show basic features of the night-time heat island that are a strong horizontal temperature gradient and a near-neutral layer of air above the urban area topped by a stable layer (Fig. 5d). In Figure 5d, it can be seen that some numerical noise still exists, despite the use of both the upstream advection scheme and horizontal diffusion. However, according to the results, this instability

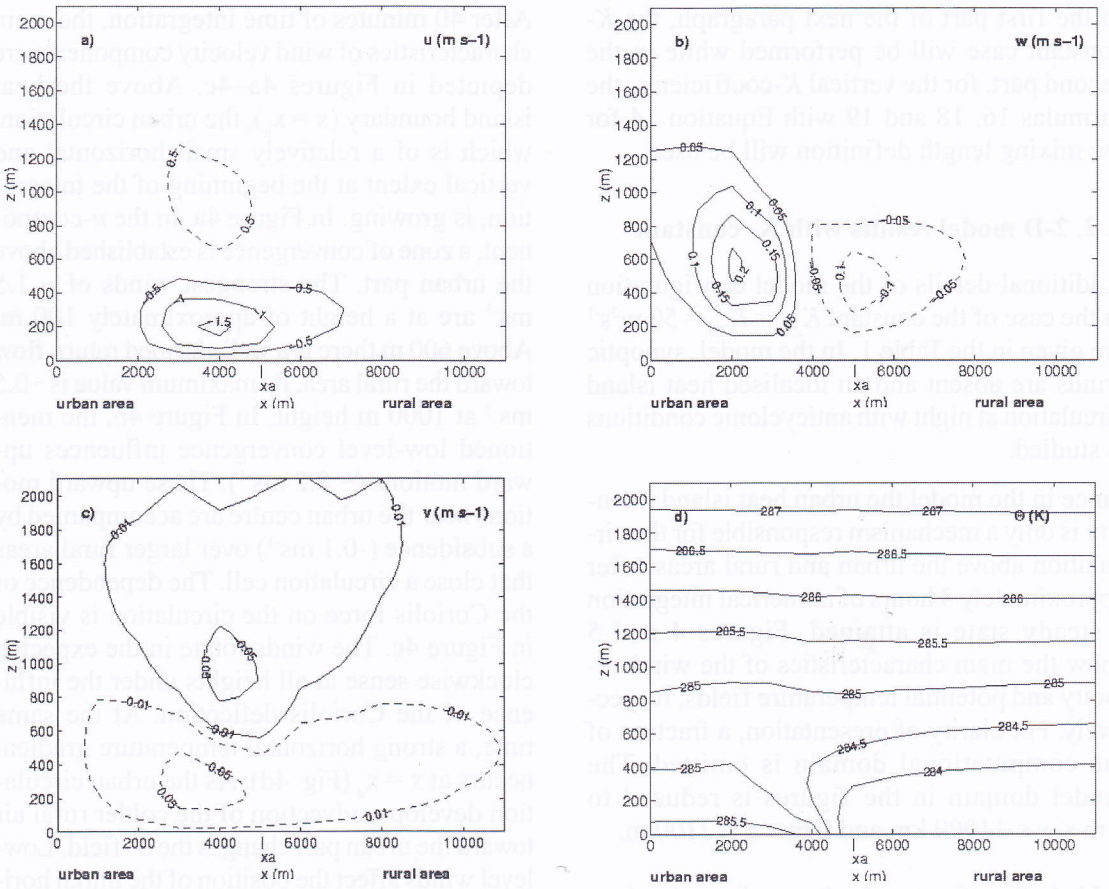

Figure 4. Results by 2-D model with constant *K*-profiles and other input parameters represented in Table 1. after 40 minutes of time integration. a) *u*-wind component (ms^{-1}); b) *w*-wind component (ms^{-1}); c) *v*-wind component (ms^{-1}) and d) potential temperature Θ (K).

Slika 4. Rezultati dvodimenzionalnog modela s konstantnim *K*-profilom i drugim ulaznim parametrima, predstavljenima u tabeli 1., nakon 40 minuta vremenske integracije. a) *u*- komponenta vjetra (ms^{-1}); b) *w*-komponenta vjetra (ms^{-1}); c) *v*- komponenta vjetra (ms^{-1}) i d) potencijalna temperatura (K).

does not change significantly the field structure.

It should be mentioned that the general features of the presented numerical simulations are in good agreement with those made by Delage and Taylor (1970). However, both the represented return flow and vertical velocity values here are more realistic, during the time integration, compared with those in Delage and Taylor (1970). In their study, they obtained almost the same values for the city-breeze flow and the return flow and *w*-values above the city centre were ~1 ms^{-1}. Tapper (1990) showed that the urban temperature excess near the ground was approximately 2.5°C (also used in the above simulation) and the return flow was started by -0.3°C at higher altitudes. This means that the return flow has to be weaker than the urban breeze, which is presented in a satisfactory way in the above simulation. Angell *et al.* (1971) examined the urban influence of Columbus in Ohio, where they found for the anticyclonic cases a maximum upward velocity of ~ 4 cms^{-1} above the city centre. Although vertical velocities in Figures 4b, 5b are slightly overestimated in comparison with the observations, they are still more realistic in relation to the Delage and Taylor (1970) model results.

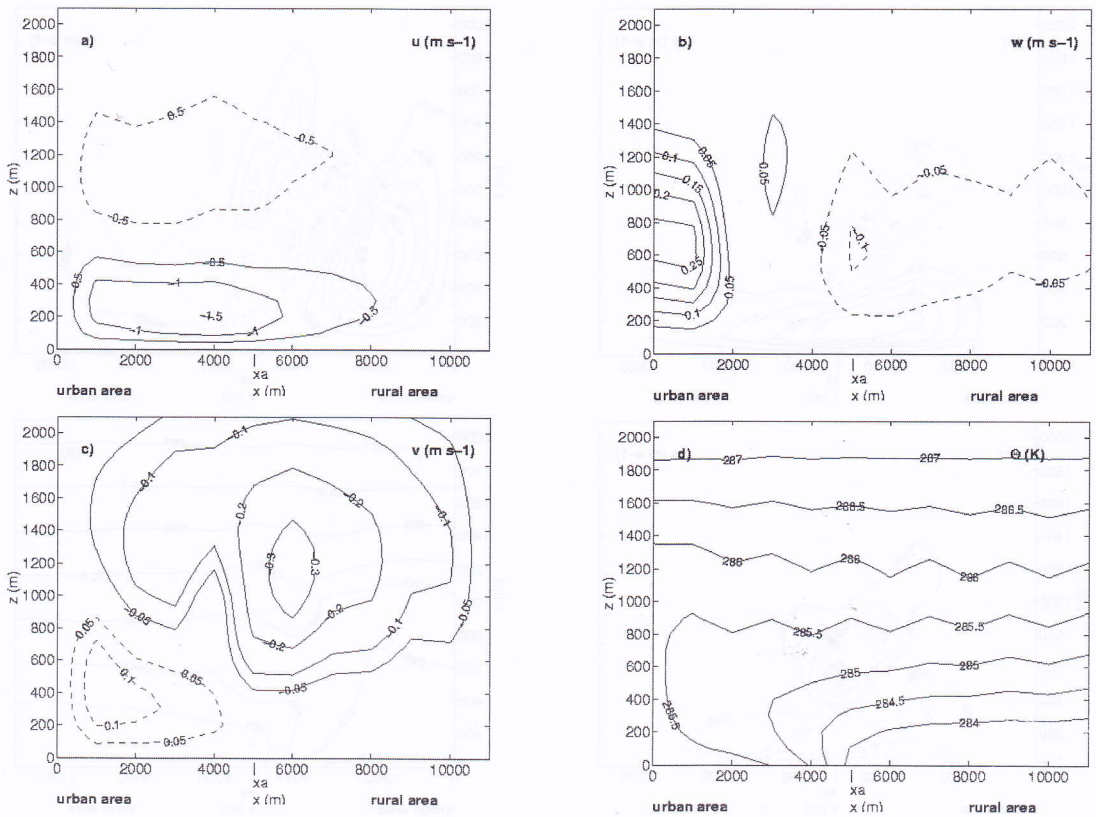

Figure 5. Same as in Figure 4 but after three hours of time integration.

Slika 5. Isto kao i na Slici 4 ali nakon tri sata vremenske integracije.

4. 3. 2-D model results with K- variable

Since we wanted to add more realism to the vertical diffusion coefficients, we implemented the D97 expressions and provided a numerical integration. As in the 1-D model, the urban boundary conditions for K_{ZM} and K_{ZH} are 0.12 and 0.16 m^2s^{-1}, respectively. For rural values, the ten-times lower magnitude for z_{0r} (see Tab. 1) has prescribed K_{ZM} = 0.012 m^2s^{-1} and K_{ZH} = 0.016 m^2s^{-1}. Computational diffusion coefficients are $K_{XM} = K_{XH} = 100$ m^2s^{-1}. In some runs, K_{XM} and K_{XH} were set equal to zero. Although the upstream advection scheme is a highly damping scheme, the use of zero value for the horizontal diffusion coefficients included numerical instability. To prevent numerical instability ($2\Delta x$ waves) to some extent and to avoid a too extensive distortion of results, we used 100 m^2s^{-1} for the horizontal eddy coefficients. Equation 14 represents the mixing length formula and varies in roughness length values for the urban and rural area defined in the Table 1. The results are similar as in the previous paragraph (4.2.) but in general the development of the circulation is a much faster process than in the *K*-constant case, of an approximate duration of one and a half an hour to approach a near-steady state. Figure 6 illustrates the urban circulation after 40 minutes of integration.

The differences in the wind component fields between the K-constant case and the D97 expressions are in the strength of the urban circulation (Figs. 6a-6d). In this case, in Figure 6a the urban and anti-urban breeze flow values are approximately 2 ms^{-1} and they follow a strong horizontal temperature gradient occurring at the urban island boundary (Fig. 6d). The urban heat island circulation extends more horizontally compared to the *K*-constant case, with no significantly changes in the circulation deepness. In Figure 6b, the upward and downward motions are higher and in Figure 6c it can be seen that the Coriolis deflection is stronger too.

Special attention is focused on the fields that are defined by D97 and describe a turbulent exchange process in the atmosphere. The alti-

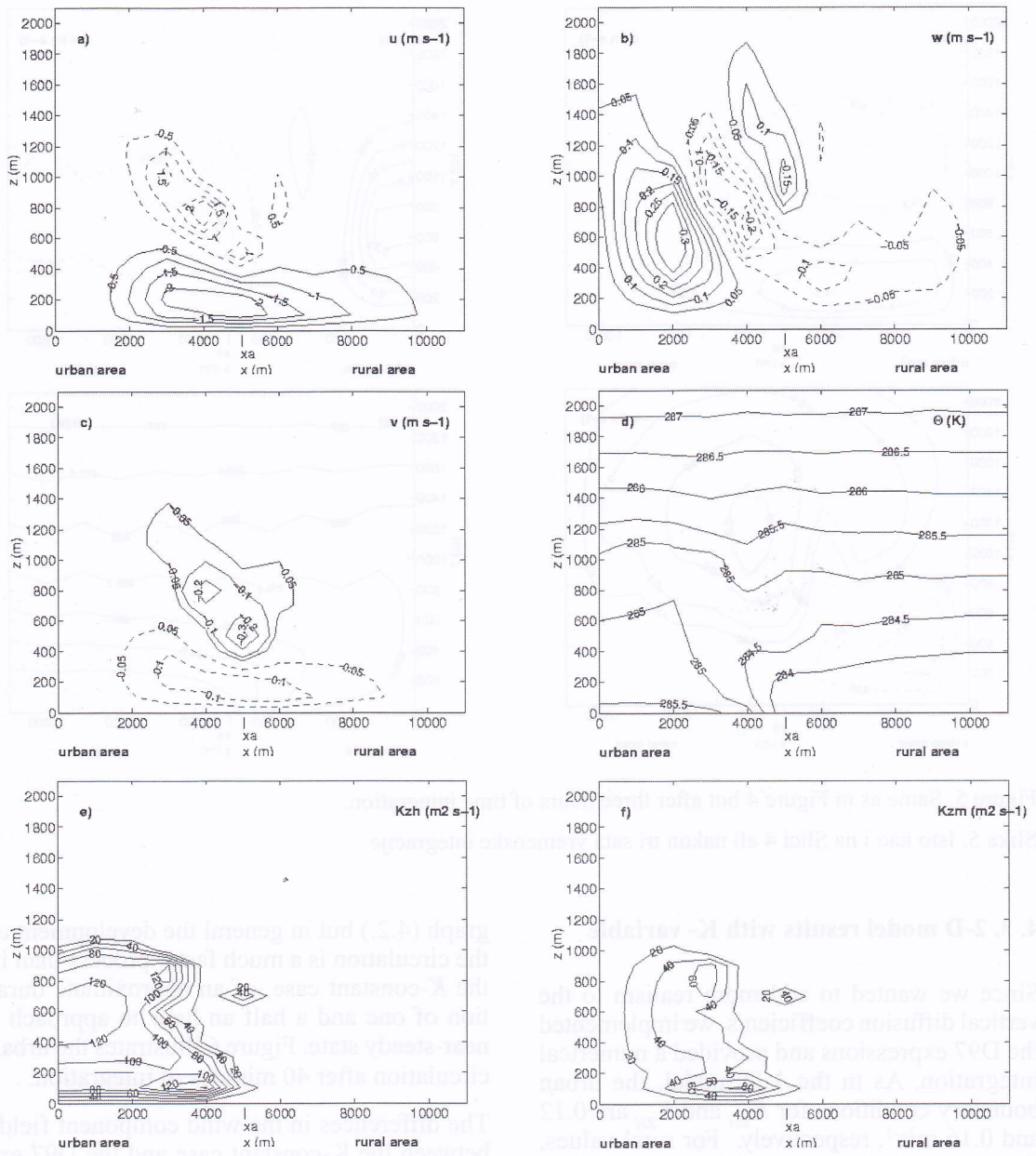

Figure 6. Results by two-dimensional model with variable K-profiles represented by Equations 14, 16, 18 and 19 and other input parameters represented in Table 1; after 40 minutes of time integration. a) u-wind component (ms^{-1}); b) w-wind component (ms^{-1}); c) v-wind component (ms^{-1}); d) potential temperature Θ (K); e) K_{ZH} coefficient (m^2s^{-1}); f) K_{ZM} coefficient (m^2s^{-1}).

Slika 6. Rezultati dvodimenzionalnog modela s vertikalno promjenjivim K-profilom predstavljenim jednadžbama 14, 16, 18 i 19 i drugim ulaznim parametrima, predstavljenima u tabeli, nakon 40 minuta vremenske integracije, a) u- komponenta vjetra (ms^{-1}); b) w- komponenta vjetra (ms^{-1}); c) v- komponenta vjetra (ms^{-1}) d) potencijalna temperatura (K); e) K_{ZH} koeficijent (m^2s^{-1}); f) K_{ZM} koeficijent (m^2s^{-1}).

tude of z_i is at about 1200 m (Fig. 6e). A turbulent mixed layer is capped by a temperature inversion. A layer of non-turbulent air lies above the inversion. Above the centre of the urban area, the height of the maximum exchange heat process is at about 500 m (~120 m^2s^{-1}). That is a somewhat overestimated result because the height of the maximum value versus z_i is usually around 1/3 (e.g. Stull, 1988). Near the urban island boundary (x_a), at 100 m height, another maximum of K_{ZH} (~140 m^2s^{-1}) is generated. There, the cold rural advection enhances

a local lapse rate over the urban–rural boundary through a small vertical extent intensifying the convection. Therefore, the advection of the cold rural air leads to a maximum flux of sensible heat. In Figure 6f, the K_{ZM} field shows maximum values of 80 and 70 m^2s^{-1} above x = 3 km at the first 200 m and 800 m height, respectively. They are due to vertical shear of the horizontal wind components inside the urban circulation (Figs. 6a, 6c). According to these results, we can conclude that K_{ZH} and K_{ZM} are capable of describing the general features of the boundary layer.

A more rapid development of the urban circulation agrees with the results obtained by the 1-D model because they show that the D97 case gives more prominent turbulent processes compared to the other cases, especially for the K_{ZH} values. The numerical integration was repeated with D70 formulas and the result was a much slower process of the circulation development and a much longer period of time required to achieve the near-steady state, compared with both D97 and K-constant cases, as we expected (see Fig. 2a). This is consistent with the results of Delage and Taylor (1970). In their model, a steady state is reached sooner, when the eddy coefficient is larger. They also reported that during the heat island development with the K variable case a transition multi-cell pattern and nodal temperature profiles above the urban part are observed. The same undesirable features are repeated in the 2-D model results presented here when both D70 and D97 cases are used. It is important to stress that although a near-steady state is attained in both cases some instability in the time integration still existed when using both D70 and D97 formulas.

Therefore, as a general comment, we can point out that D97 has certain weaknesses during the numerical modelling of a mesoscale phenomenon such as urban heat island circulation. Despite the physically correct treatment of free convection, the new D97 approach has not significantly improved numerical simulations compared to the D70 case. The use of the K-constant case has given much better results although this case has serious physical weaknesses.

5. CONCLUDING REMARKS

This modelling study has tried to evaluate Equations 1–3, which characterise turbulent exchange processes in the surface layer, in the simple 1-D and 2-D numerical models. In the first part of the paper, the 1-D model shows some characteristics of the stability functions, represented by Equations 1–3. The investigated functions represent more prominent turbulent processes than the K-constant, D70 and O'Brien cases. In the second part, the ability of the mentioned functions to provide a successful integration of the urban heat island circulation is examined. Although these functions are very attractive in the context of global atmospheric circulation models, they did not successfully describe the development of the urban heat island circulation. The following may be regarded as plausible reasons:

- In the 2-D model, the ordinary upstream advection scheme and the computational diffusion are used. However, in the model results $2\Delta x$ waves still exist and some additional filters have to be applied.
- Stull (1991) pointed out that static stability should not be evaluated on the basis of the local lapse rate. Considering only the local lapse rate, this leads to improper conclusions. He suggested a non-local determination of static stability that accounts for both the local lapse rate and convective air parcels moving across finite distances.
- The *K*-theory assumes that fluxes are associated with only small size eddies (which is not the case in free convection) and represent unrealistic interpretations of the physics of flows with large eddies. The eddy diffusivities arise out of a first order turbulence closure that is essentially local. The urban heat island circulation is of too large a scale to make this a reasonable approach.
- Applying MOST for the parameterisation of surface layer fluxes for conditions of extreme stratification, the theory can give a quite uncertain approximation of the turbulent fluxes (e.g. Weidinger *et al.*, 2000).

However, it remains moot whether efforts can improve greatly the inherent uncertainties and errors associated with the current methods summarised above. The simulations presented here are very simplified, but this approach, however, allows us to study Equations 1–3 more systematically. We can presumably improve the present numerical 2-D results with the implementation of a turbulent kinetic energy equation but this can be the subject of further studies.

APPENDIX A

In the 1-D model, the finite difference analogs of Equations 9–11 are in the staggered grid with a constant vertical grid interval because staggering increases the effective resolution according to e.g. Pielke (1984). The model has only a vertical coordinate where the origin of the grid system is situated at the ground and the top of the model domain at $z\,(N) = H$. The coordinate of the vertical grid points for u, v, and Θ are denoted by $z(i)$ and for K_{ZM} and K_{ZH} by $zm(i)$. These two grid discretizations are connected in such a way that $zm(i)$ is equal to $z(i\text{-}1/2)$ and $zm(i+1)$ to $z(i+1/2)$ (see Fig. 1).

Equation 9 for u-velocity is:

$$\frac{u(n+1,i)-u(n,i)}{\Delta t} = fv(n,i) + \frac{K_{ZM\,(i+(1/2))}}{(\Delta z)^2}u(n,i+1) - \frac{(K_{ZM\,(i+(1/2))} + K_{ZM\,(i-(1/2))})}{(\Delta z)^2}u(n,i) + \\ + \frac{K_{ZM\,(i-(1/2))}}{(\Delta z)^2}u(n,i-1) \tag{A1}$$

for v-velocity (Eq. 10) is:

$$\frac{v(n+1,i)-v(n,i)}{\Delta t} = -f(\alpha_1 u(n,i) + \alpha_2 u(n+1,i)) + \frac{K_{ZM\,(i+(1/2))}}{(\Delta z)^2}v(n,i+1) - \\ - \frac{(K_{ZM\,(i+(1/2))} + K_{ZM\,(i-(1/2))})}{(\Delta z)^2}v(n,i) + \frac{K_{ZM\,(i-(1/2))}}{(\Delta z)^2}v(n,i-1) \tag{A2}$$

and Equation 11 for potential temperature is:

$$\frac{\Theta(n+1,i)-\Theta(n,i)}{\Delta t} = \frac{K_{ZH\,(i+(1/2))}}{(\Delta z)^2}\Theta(n,i+1) - \frac{(K_{ZH\,(i+(1/2))} + K_{ZH\,(i-(1/2))})}{(\Delta z)^2}\Theta(n,i) + \\ + \frac{K_{ZH\,(i-(1/2))}}{(\Delta z)^2}\Theta(n,-1) \tag{A3}$$

where the following notation is used: n = integer time step, i = integer grid point on the z-axis, Δt = time step, Δz = constant grid interval on z-axis. The Coriolis terms are calculated by an implicit scheme (Pielke, 1984); in Equation A2, an updated value for u is used (from Eq. A1), which can be controlled by the coefficients α_1 and α_2. Values $\alpha_1 = 0$ and $\alpha_2 = 1$ are used here.

APPENDIX B

In the 2-D model, the finite difference analogs of Equations 4–8 with the aid of a grid system on the x-z plane are presented and a variable vertical grid interval is used. Here, we consider the calculations of flow above the surface whose properties vary along the x-axis and z-axis. The coordinates of the vertical grid points are denoted by $z(j)$. The origin of the grid system is situated at the ground, in the centre of the urban area, ($x\,(1) = 0$ and $z\,(1) = 0$). Another lateral boundary is situated at $x(M) = L$ and the top of the model domain at $z(N) = H$.

Equation 4 for u velocity is:

$$\frac{u(n+1,i,j)-u(n,i,j)}{\Delta t} = -u(n,i,j)\frac{(u(n,i,j)-u(n,i-l,j))\cdot l}{\Delta x} - w(i,j)\frac{(u(n,i,j)-u(n,i,j-l))\cdot l}{(z(j)-z(j-l))\cdot l} + fv(n,i,j)$$
$$-\frac{R\cdot\Theta(n,i,j)}{p(i,j)}\frac{p(i+1.j)-p(i-1,j)}{2\Delta x}\left(\frac{p(i.j)}{p_0}\right)^{R/Cp} + \frac{K_{ZM}(i,j+1)+K_{ZM}(i,j)}{z(j+1)-z(j-1)}\cdot\beta_1\cdot\frac{u(n,i,j+1)-u(n,i,j)}{z(j+1)-z(j)}$$
$$+\frac{K_{ZM}(i,j+1)+K_{ZM}(i,j)}{z(j+1)-z(j-1)}\cdot\beta_2\cdot\frac{u(n+1,i,j+1)-u(n+1,i,j)}{z(j+1)-z(j)} - \frac{K_{ZM}(i,j)+K_{ZM}(i,j-1)}{z(j+1)-z(j-1)}\cdot\beta_1\cdot\frac{u(n,i,j)-u(n,i,j-1)}{z(j)-z(j-1)}$$
$$-\frac{K_{ZM}(i,j)+K_{ZM}(i,j-1)}{z(j+1)-z(j-1)}\cdot\beta_2\cdot\frac{u(n+1,i,j)-u(n+1,i,j-1)}{z(j)-z(j-1)} + \frac{K_{XM}\cdot(u(n,i+1,j)+u(n,i-1,j)-2u(n,i,j))}{(\Delta x)^2} \quad \text{(B1)}$$

for v velocity (eq. 5) is:

$$\frac{v(n+1,i,j)-v(n,i,j)}{\Delta t} = -u(n,i,j)\frac{(v(n,i,j)-v(n,i-l,j))\cdot l}{\Delta x} - w(i,j)\frac{(v(n,i,j)-v(n,i,j-l))\cdot l}{(z(j)-z(j-l))\cdot l} - fu(n+1,i,j)$$
$$+\frac{K_{ZM}(i,j+1)+K_{ZM}(i,j)}{z(j+1)-z(j-1)}\cdot\beta_1\cdot\frac{v(n,i,j+1)-v(n,i,j)}{z(j+1)-z(j)} + \frac{K_{ZM}(i,j+1)+K_{ZM}(i,j)}{z(j+1)-z(j-1)}\cdot\beta_2\cdot\frac{v(n+1,i,j+1)-v(n+1,i,j)}{z(j+1)-z(j)}$$
$$-\frac{K_{ZM}(i,j)+K_{ZM}(i,j-1)}{z(j+1)-z(j-1)}\cdot\beta_1\cdot\frac{v(n,i,j)-v(n,i,j-1)}{z(j)-z(j-1)} - \frac{K_{ZM}(i,j)+K_{ZM}(i,j-1)}{z(j+1)-z(j-1)}\cdot\beta_2\cdot\frac{v(n+1,i,j)-v(n+1,i,j-1)}{z(j)-z(j-1)}$$
$$+\frac{K_{XM}\cdot(v(n,i+1,j)+v(n,i-1,j)-2v(n,i,j))}{(\Delta x)^2} \quad \text{(B2)}$$

and equation 6 for potential temperature is:

$$\frac{\Theta(n+1,i,j)-\Theta(n,i,j)}{\Delta t} = -u(n,i,j)\frac{(\Theta(n,i,j)-\Theta(n,i-l,j))\cdot l}{\Delta x} - w(i,j)\frac{(\Theta(n,i,j)-\Theta(n,i,j-l))\cdot l}{(z(j)-z(j-l))\cdot l}$$
$$+\frac{K_{ZH}(i,j+1)+K_{ZH}(i,j)}{z(j+1)-z(j-1)}\cdot\beta_1\cdot\frac{\Theta(n,i,j+1)-\Theta(n,i,j)}{z(j+1)-z(j)} + \frac{K_{ZH}(i,j+1)+K_{ZH}(i,j)}{z(j+1)-z(j-1)}\cdot\beta_2\cdot\frac{\Theta(n+1,i,j+1)-\Theta(n+1,i,j)}{z(j+1)-z(j)}$$
$$-\frac{K_{ZH}(i,j)+K_{ZH}(i,j-1)}{z(j+1)-z(j-1)}\cdot\beta_1\cdot\frac{\Theta(n,i,j)-\Theta(n,i,j-1)}{z(j)-z(j-1)} - \frac{K_{ZH}(i,j)+K_{ZH}(i,j-1)}{z(j+1)-z(j-1)}\cdot\beta_2\cdot\frac{\Theta(n+1,i,j)-\Theta(n+1,i,j-1)}{z(j)-z(j-1)}$$
$$+\frac{K_{XH}\cdot(\Theta(n,i+1,j)+\Theta(n,i-1,j)-2\Theta(n,i,j))}{(\Delta x)^2} \quad \text{(B3)}$$

where the following notation is used: n = integer time step, i = integer grid point on the x-axis, j = integer grid point on the z-axis, Δt = time step, Δx = grid interval on the x-axis, l index used in the upstream finite differences

$l = 1$ for $u(i,j) > 0$ and $w(i,j) > 0$ and $l = -1$ otherwise.

In (B1)–(B3), for local tendencies and horizontal diffusion terms, forward in time and central difference schemes are utilised, respectively. The ordinary upstream finite differences (i.e. 1st order accuracy in space and time) approximate the advective terms to avoid numerical instabilities. Semi-implicit treatment of the vertical diffusion terms in these equations is visible in the weight parameters $ß_1$ and $ß_2$ which determine current and future contributions to the numerical approximation (Pielke, 1984). Here $ß_1 = 0.25$ and $ß_2 = 0.75$, since Pielke (1984) also mentioned that this choice of parameters provides a representation as accurate as the explicit scheme but with a much longer permissible time step. The Coriolis terms are calculated by an implicit scheme as in the 1-D model (Pielke, 1984).

Equation 7 is written according to Kozo (1982) and it is used to compute w after every time step using new u velocity. The integration proceeds upward from the surface and needs only one boundary condition for w; $w = 0$ at the ground:

$$w(i,j) = w(i,j-1) - \frac{(z(j)-z(j-1))}{4\Delta x}(u(n+1,i+1,j-1)-u(n+1,i-1,j-1)+u(n+1,i+1,j)-u(n+1,i-1,j)) \quad \text{(B4)}$$

Estoque (1961) has already pointed out that in the case of two boundary conditions (i.e. $w = 0$ for $z = 0$ and $z = H$) the results of the velocity and temperature fields would be distorted to a certain degree.

In order to compute the pressure Equation 8 is represented as (Koračin, 1997, personal communication):

$$p(i,j) = \left((p(i,j+1))^{R/Cp} + \frac{2 \cdot g \cdot (z(j+1) - z(j)) \cdot p_0^{R/Cp}}{Cp \cdot (\Theta(n,i,j+1) + \Theta(n,i,j))} \right)^{Cp/R} \quad \text{(B5)}$$

The pressure integration proceeds downward from the top of the model domain toward the bottom.

Acknowledgements: *The authors are highly grateful to Dr.Sc. Nadežda and Dr.Sc. Yves Delage for their invaluable advice and assistance during many phases of this work. The 1-D model development has been provided during the postgraduate course (Atmospheric Modelling, 1999) thanks to Dr.Sc. Darko Koračin and postgraduate students. Many thanks to Mr.Sc. Ivica Sović for his constructive discussion of details in the development of the model's code and the referee who offered suggestions, which considerably improved the paper.*

REFERENCES

Angell, J. K., D. H. Pack, C. R. Dickson and W. H. Hoecker, 1971: Urban influence on nighttime airflow estimated from Tetroon flights. *J. Appl. Meteor.*, **10**, 194–204.

Blackadar, A. K., 1962: The vertical distribution of wind and turbulent exchange in a neutral atmosphere. *J. Geophys. Res.*, **67**, 3095–3102.

Businger, J. A., J. C. Wyngaard, Y. Izumi and E. F. Bradley, 1971: Flux-profile relationships in the atmospheric surface layer. *J. Atmos. Sci.*, **28**, 181–189.

Cvitan, L., 1991: Profil vjetra u prizemnom graničnom sloju atmosfere. *Hrv. meteor. časopis* **26**, 53–64.

Delage, Y. and P. A. Taylor, 1970: Numerical studies of heat island circulations. *Boundary-Layer Meteor.*, **1**, 201–226.

Delage, Y. and C. Girard, 1992: Stability functions correct at the free convection limit and consistent for both the Surface and Ekman layers. *Boundary-Layer Meteor.*, **58**, 19–31.

Delage, Y., 1997: Parameterising sub-grid scale vertical transport in atmospheric models under statically stable conditions. *Boundary-Layer Meteor.*, **82**, 23–48.

Estoque, M. A., 1961: A theoretical investigation of the sea breeze. *Quart. J. Roy. Meteor. Soc.*, **87**, 136–146.

Högström, U., 1988: Non-dimensional wind and temperature profiles in the atmospheric surface layer: A re-evaluation. *Boundary-Layer Meteor.*, **42**, 55–78.

Kalnay E. and M. Kanamitsu, 1988: Time schemes for strongly nonlinear damping equations. *Mon. Wea. Rev.*, **116**, 1945–1958.

Kozo, T. L., 1982: A mathematical model of sea breezes along the Alaskan Beaufort Sea Coast: Part II. *J. Appl. Meteor.*, **21**, 906–924.

Louis, J. F., 1979: A parametric model of vertical eddy fluxes in the atmosphere. *Boundary-Layer Meteor.*, **17**, 187–202.

O'Brien, J. J., 1970: A note on the vertical structure of the eddy exchange coefficient in the Planetary Boundary Layer. *J. Atmos. Sci.*, **30**, 1213–1215.

Pielke, R. A., 1984: Mesoscale meteorological modeling. Academic Press, Orlando. 612 pp.

Stull, R. B., 1988: An introduction to boundary layer meteorology. Kluwer, Dordrecht, 666 pp.

Stull, R. B., 1991: Static stability-An update. *Bull. Amer. Meteor. Soc.*, **72**, 1521–1529.

Tapper, N. J., 1990: Urban influence on boundary layer temperature and humidity: Results from Christchurch, New Zealand. *Atmos. Environ.*, **26B**, 19–27.

Vukovich, F. M., J. W. Dunn and B. W. Crissman 1976: A theoretical study of the St. Louis heat island: the wind and temperature distribution. *J. Appl. Meteor.*, **15**, 417–440.

Weidinger, T., J. Pinto and L. Horwáth, 2000: Effects of uncertainties in universal function, roughness length, and displacement height on the calculation of surface layer fluxes. *Meteor. Z. N. F.*, **9**, 139–154.